Polyhedron 87 (2015) 71–78

Contents lists available at ScienceDirect

Polyhedron

journal homepage: www.elsevier.com/locate/poly

Rapid mechanochemical protocol for isostructural polycatenated coordination polymers [M(**BrIP**)(**BIX**)] (M = Co(II), Zn(II))

Kamal Kumar Bisht [a,b,c,*], Jayesh Chaudhari [a], Eringathodi Suresh [a,b,*]

[a] Analytical Discipline and Centralized Instrument Facility, CSIR–Central Salt and Marine Chemicals Research Institute, Council of Scientific and Industrial Research, G.B. Marg, Bhavnagar 364002, Gujarat, India
[b] Academy of Scientific and Innovative Research (AcSIR), CSIR–Central Salt and Marine Chemicals Research Institute, Council of Scientific and Industrial Research, G.B. Marg, Bhavnagar 364002, Gujarat, India
[c] Department of Chemistry, University of Petroleum and Energy Studies (UPES), P.O. Bidholi Via-Prem Nagar, Dehradun 248007, Uttarakhand, India

ARTICLE INFO

Article history:
Received 7 September 2014
Accepted 15 October 2014
Available online 4 November 2014

Keywords:
Coordination polymer
Liquid assisted grinding
Mechanochemistry
Isostructural
Interpenetration

ABSTRACT

Two dual ligand isostructural coordination polymers [Co(**BrIP**)(**BIX**)]$_n$ (**1**) and [Zn(**BrIP**)(**BIX**)]$_n$ (**2**), where **BrIP** = 5-bromoisophthalate and **BIX** = 1,4-bis(imidazol-1-ylmethyl)-benzene, have been efficiently synthesized by liquid assisted grinding methods. Single crystals of **1** were harvested by the solvothermal technique and phase pure **1** or **2** can be quantitatively obtained by grinding equimolar amounts of the metal nitrates and the ligands, 5-bromoisophthalic acid (H_2**BrIP**) and 1,4-bis(imidazol-1-ylmethyl)-benzene (**BIX**) in the presence of a few drops of water or methanol. Use of freshly prepared $Co(OH)_2$ or ZnO also yields the desired end products in an environmentally friendly manner along with the benign by-product water. The structure of **1** was established by single crystal X-ray diffraction studies, in addition to other physicochemical techniques. Morphological aspects of samples of **1** and **2** obtained *via* different protocols have also been studied.

1. Introduction

Mechanochemistry, emerging as an efficient alternative to conventional approaches, is becoming increasingly popular in multidisciplinary research areas and major emphasis is being paid to the implementation of mechanochemical processes towards the time and energy efficient syntheses of a variety of materials, including metal organic framework (MOF)/coordination polymer (CP) co-crystals, Active Pharmaceutical Ingredients (APIs), metal oxides etc. [1,2]. Efforts are also being made to improve the mechanistic understanding of such processes to gain control over important aspects, such as the phase purity of the desired substances [3,4].

In the context of MOFs/CPs, solvothermal and other solution based methods are the mainstream routes; however, recently significant attention is being paid to non-conventional synthetic methods, which include mechanochemistry, sonochemistry, microwave irradiation and new techniques such as 'accelerated aging' [5]. Particularly, mechanochemical (milling or grinding) reactions are an efficient and environmentally green alternative for the synthesis of MOFs due to advantages such as a low energy requirement, less time consumption and minimal solubility issues [2,6]. A decade ago, Steed and co-workers reported the first ever CP synthesized by manual grinding of copper acetate and the ligand 1,3-di-4-pyridylpropane [7]. Subsequently, the popularity of mechanochemical methods for achieving CPs increased, which reflects in remarkable work of Braga, James and other groups [8]. The presence of minute amounts of liquids or ionic species during the course of the mechanochemical reaction may facilitate the synthetic conversion of the precursors to the desired products with enhanced selectivity, reaction rate and yield. These liquid assisted grinding (LAG) and ion assisted grinding (IAG) techniques have recently been implemented for the synthesis of a variety of substances, including MOF synthesis [9,1b]. Recently, Friščić has discussed mechanochemical approaches to synthesize CPs and other supramolecular architectures in an excellent tutorial review [10].

There are plenty of reports on ternary CPs synthesized *via* solution based methods [11]. Significant progress towards the mechanochemical synthesis of CPs comprising of only one kind of ligand has also been achieved [6a]. However, on the contrary, dual ligand CPs have rarely been synthesized by mechanochemical approaches [6a,12]. An exemplary report by Friščić and Fabian establishes the

* Corresponding authors at: Analytical Discipline and Centralized Instrument Facility, CSIR–Central Salt and Marine Chemicals Research Institute, Council of Scientific and Industrial Research, G.B. Marg, Bhavnagar 364002, Gujarat, India.
E-mail addresses: kkbisht@ddn.upes.ac.in (K.K. Bisht), sureshe123@rediffmail.com, esuresh@csmcri.org (E. Suresh).

http://dx.doi.org/10.1016/j.poly.2014.10.029
0277-5387/

single step mechanochemical fabrication of zinc fumarate networks pillared by 4,4′-dipyridyl or trans-1,2-bis(4-pyridyl)-ethylene ligands [12].

Interpenetration or catenation of networks in CPs is an interesting feature, not only for the intrigue geometrical aspects but also for the impact of interlocked networks on properties such as selective separation and adsorption [10,13]. Mechanochemical (liquid assisted grinding) synthesis of discrete interlocked structures has recently been explored by Koshkakaryan et al. for the donor–acceptor stacks of crown ether and naphthalene diimide [13a]. In this sequence, we are not aware of any report describing the mechanochemical synthesis of interpenetrated ternary MOFs which would practically extend the scope of mechanochemical methodologies towards the realization of more intricate metal organic architectures (Schemes 1 and S1) [14].

Herein we report on the synthesis of interpenetrated mixed ligand CPs *via* a liquid assisted grinding approach (Scheme 1). The dual ligand CP, [Co(**BrIP**)(**BIX**)]$_n$ (**1**) was prepared by mechanochemical as well as hydrothermal methods and established by single crystal, powder X-ray diffraction and other physicochemical methods. The crystal structure of [Co(**BrIP**)(**BIX**)]$_n$ reveals a rare threefold polycatenated 2D → 3D parallel interpenetrated network which is isostructural to a known CP, [Zn(**BrIP**)(**BIX**)]$_n$ (**2**) [15]. A series of solvent-free and liquid assisted grinding experiments were performed to optimize the synthesis of these intricate Co/Zn CPs in time and energy efficient manners. To the best of our knowledge we are unaware of any parallel report on the mechanochemical synthesis of multiple ligand MOFs possessing intricate structural features such as interpenetrated or polycatenated networks.

2. Experimental

2.1. General

Reagents for the synthesis of the ligands **BIX** and H_2**BrIP** were purchased from Sigma–Aldrich. Metal salts and organic solvents were obtained from RANBAXY laboratories limited and SD Fine Chemicals, India. $Co(OH)_2$ was prepared according to a reported procedure [16a]. Distilled water was used for the synthetic manipulations. All the reagents and solvents were used as received without any further purification. The ligands **BIX** and H_2**BrIP** were synthesized by following reported procedures [16b,c]. CHNS analyses were done using a Perkin–Elmer 2400 CHNS/O analyzer. IR spectra were recorded using KBr pellets on a Perkin–Elmer GX FTIR spectrometer. For each IR spectra 10 scans were recorded at 4 cm^{-1} resolution. TGA analysis was carried out using Mettler Toledo Star SW 8.10. Solid state UV–Vis spectra and luminescence spectra were recorded using a Shimadzu UV-3101PC spectrometer and a Fluorolog Horiba JobinYvon spectrophotometer respectively. The SEM (Leo series 1430 VP) equipped with INCA Energy EDS was used to examine the textural features of the samples. PXRD data were collected at a rate of 0.05°/s on a PANalytical Empyrean (PIXcel 3D detector) diffractometer with a combination of 1/16° divergence and 1/32° anti scatter slits. Rietveld refinements were performed against the single crystal data using HIGHSCORE PLUS software (PANalytical). Single crystal structures were determined using a BRUKER SMART APEX (CCD) diffractometer. A summary of the crystallographic data and details of the single crystal X-ray diffraction data collection for **1** are given in Table 1.

2.2. Solvothermal synthesis of *1*

$Co(NO_3)_2{\cdot}6H_2O$ (54 mg, 0.18 mmol), H_2**BrIP** (45 mg, 0.18 mmol), **BIX** (90 mg, 0.37 mmol) and 9.5 mL of distilled water in a 23 mL Teflon-lined vessel were hydrothermally reacted at 398 K for 50 h and then cooled slowly to room temperature. A violet colored crystalline material along with X-ray quality crystals were obtained. The material was isolated in 57% yield after washing with distilled water and methanol, and drying in air. Elemental analysis (%): Calc.: C, 48.91; H, 3.17; N, 10.37; Obs.: C, 48.73; H, 3.32; N, 10.04. FTIR cm^{-1} (KBr): 3436 (br), 3097 (m), 2369 (w), 1617 (s), 1560 (m), 1428 (w), 1345 (s), 1244 (w), 1103 (m), 1027 (w), 951 (w), 889 (w), 766 (m), 733 (s), 660 (w), 444 (w).

2.3. Procedure for the mechanochemical syntheses

In a typical mechanochemical reaction, 0.09 mmol of each reactant, i.e. 27 mg of $Co(NO_3)_2.6H_2O$ (or 9 mg of $Co(OH)_2$ or 27 mg of $Zn(NO_3)_2{\cdot}6H_2O$ or 8 mg of ZnO), 23 mg of H_2**BrIP** and 22 mg of **BIX**, were taken in a mortar and gently kneaded with a pestle for 30–45 min at ambient temperature. The desired crystalline product was obtained by the hydrothermal method when the metal salt:H_2**BrIP**:**BIX** ratio was 1:1:2; however, the mechanochemical syntheses were executed with 1:1:1 reactants stoichiometry. The obtained material was allowed to stand overnight in an ambient atmosphere. In the case of liquid assisted grinding (LAG), 100 μL solvent (water or methanol) was added to the dry reactants before grinding was commenced and kneading was performed for 15–30 min. A color change was observed in all cases with an increase in grinding time and a violet colored homogeneous powder was obtained on completion of the reactions. Thus, $_{Nitrate}\mathbf{1}^{\mathbf{Neat}}$, $_{Nitrate}\mathbf{1}^{\mathbf{MeOH}}$, $_{Hydroxide}\mathbf{1}^{\mathbf{H_2O}}$, $_{Nitrate}\mathbf{1}^{\mathbf{H_2O}}$, $_{Nitrate}\mathbf{2}^{\mathbf{H_2O}}$ and $_{Oxide}\mathbf{2}^{\mathbf{H_2O}}$ were synthesized, where the subscripts 'Nitrate', 'Hydroxide' or 'Oxide' indicate the anion of metal salts used and the superscripts 'Neat', 'MeOH' or 'H_2O' represent the solvent-free, methanol or water assisted kneading processes respectively. Thus, the subscripts and superscripts in the designated samples are used as identity to the metal precursor and grinding protocol respectively. The prepared samples were characterized by PXRD and FTIR analyses.

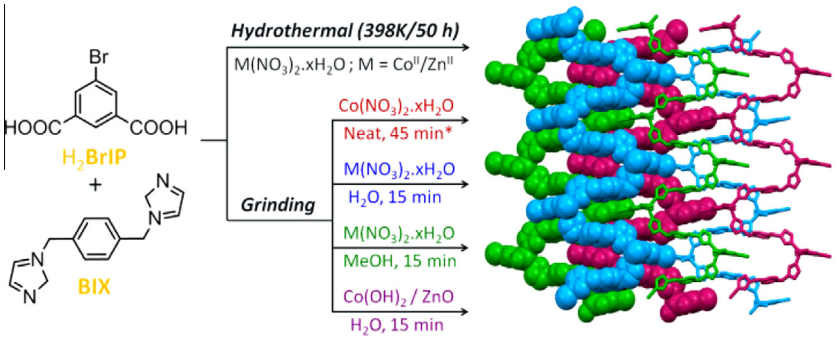

Scheme 1. Hydrothermal and various grinding reactions between the ligands (H_2**BrIP**/**BIX**) and metal precursors yield the interpenetrated ternary coordination polymers **1** and **2**.

Table 1
Crystal data and structure refinement for **1**.

Identification code	**1**
Chemical formula	$C_{22}H_{17}BrCoN_4O_4$
Formula weight	540.24
Crystal color	violet
Crystal size (mm)	0.30 × 0.08 × 0.04
Temperature (K)	150(2)
Crystal system	monoclinic
Space group	$P2_1/c$
a (Å)	10.1762(10)
b (Å)	14.3672(13)
c (Å)	14.6236(14)
α (°)	90
β (°)	106.034(2)
γ (°)	90
Z	4
V (Å^3)	2054.8(3)
Density (Mg/m^3)	1.746
Absorption coefficient (mm^{-1})	2.819
F(000)	1084
Reflections collected	11983
Independent reflections	4627
$R_{(int)}$	0.0264
Number of parameters	357
S (Goodness-of-fit (GOF)) on F^2	1.030
Final R_1/wR_2 ($I > 2\sigma(I)$)	0. 0.0359/0.0843
Weighted R_1/wR_2 (all data)	0. 0.0431/0.0875
CCDC number	943102

$R = \Sigma||Fo| - |Fc||/\Sigma|Fo|$; $wR = [\Sigma w(Fo^2 - Fc^2)^2/\Sigma w(Fo^2)^2]^{1/2}$.

Experimental elemental analysis did not show results consistent with calculated values due to varying minute amounts of the unreacted precursors. However, the samples prepared by LAG followed by washing with methanol or acetone showed expected elemental composition.

Nitrate $\mathbf{1}^{\mathbf{Neat}}$*:* Kneading time: 45 min; Yield: >92%; FTIR (KBr): 3415 (br), 3132 (s), 2842 (w), 2628 (w), 1921 (w), 1704 (w), 1614 (m), 1553 (m), 1386 (s), 1316 (s), 1092 (w), 1040 (w), 948 (w), 897 (w), 827 (w), 756 (w), 715 (m), 624 (w), 448 (w).

Nitrate $\mathbf{1}^{\mathbf{MeOH}}$*:* Kneading time: 15 min; Yield: 94%; Calc. for $C_{22}H_{17}BrCoN_4O_4$: C, 48.91; H, 3.17; N, 10.37; Obs. for washed sample: C, 48.78; H, 3.32; N, 10.12.; FTIR (KBr):3376 (br), 3132 (w), 3098 (w), 2961 (w), 2830 (w), 2717 (w), 2617 (w), 2358 (w), 1932 (w), 1704 (w), 1619 (s), 1551 (m), 1409 (s), 1340 (s), 1096 (m), 1031 (w), 955 (w), 892 (w), 841 (w), 755 (m), 733 (m), 660 (w), 626 (w), 444 (w).

Hydroxide $\mathbf{1}^{\mathbf{H_2O}}$*:* Kneading time: 15 min; Yield: ~92%; FTIR (KBr): 3321 (br), 3121 (m), 1618 (s), 1554 (m), 1427 (w), 1341 (s), 1100 (m), 1027 (w), 953 (w), 887 (w), 759 (m), 731 (s), 658 (w), 447 (w).

Nitrate $\mathbf{1}^{\mathbf{H_2O}}$*:* Kneading time: 15 min; Yield: 93%; FTIR (KBr): 3427 (br), 3099 (m), 2362 (w), 1618 (s), 1551 (m), 1429 (w), 1343 (s), 1247 (w), 1102 (m), 1020 (w), 953 (w), 885 (w), 765 (m), 732 (s), 659 (w), 444 (w).

Nitrate $\mathbf{2}^{\mathbf{H_2O}}$*:* Kneading time: 15 min; Yield: 94%; Calc. for $C_{22}H_{17}BrZnN_4O_4$: C, 48.33; H, 3.13; N, 10.25; Obs. after washing: C, 48.14; H, 3.29; N, 10.17. FTIR (KBr): 3426 (br), 3101 (s), 3027 (w), 2374 (w), 1627 (s), 1564 (m), 1526 (w), 1425 (w), 1341 (s), 1244 (w), 1173 (w), 1104 (m), 1025 (w), 954 (w), 893 (w), 766 (m), 734 (s), 659 (w), 443 (w).

Oxide $\mathbf{2}^{\mathbf{H_2O}}$*:* Kneading time: 15 min; Yield: ~91%; FTIR (KBr): 3434 (br), 1623 (s), 1559 (m), 1525(w), 1344 (s), 1245 (w), 1181 (w), 1107 (m), 1023 (w), 954 (w), 889 (w), 766 (m), 735 (s), 657 (w), 441 (w).

2.4. X-ray crystallography

Summaries of the crystallographic data, details of hydrogen bonding interactions and selected bond lengths and bond angles for **1** are given in Tables 1, 2 and S1 respectively. A single crystal with ideal dimensions was transferred rapidly from the mother liquor and immersed in paratone oil before being mounted for data collection at 150 K. Intensity data for the crystal was collected using MoK$_\alpha$ (λ = 0.71073 Å) radiation on a Bruker SMART APEX diffractometer equipped with a CCD area detector. The data integration and reduction were processed with the SAINT software [17a]. An empirical absorption correction was applied to the collected reflections with SADABS [17b]. The structure was solved by direct methods using SHELXTL and were refined on F^2 by the full-matrix least-squares technique using the program SHELXL-97 [17c,d]. All non-hydrogen atoms were refined anisotropically until convergence was reached. Hydrogen atoms attached to the organic moieties were either located from the difference Fourier map or stereochemically fixed.

3. Results and discussion

3.1. Crystal and molecular structure of *1* and *2*

1 crystallizes in the monoclinic system, $P2_1/c$ space group with one Co(II) ion, one **BrIP** and one **BIX** ligand constituting the asymmetric unit, as presented in Fig. 1. Crystallographic analysis revealed that two units of each **BrIP** and **BIX** moiety provide an N_2O_2 coordination environment around the Co(II) ions in a distorted tetrahedral geometry. **BrIP** exhibits the $\mu_2\eta^1{:}\eta^1$-coordination mode, bridging Co(II) centers with a separation of 10.17 Å and generating linear {Co(II)**BrIP**}$_n$ chains (Fig. 2a). Linear {Co(II)**BrIP**}$_n$ chains oriented along the *a*-axis are cross linked *via* **BIX** ligands (along the *b*-axis) generating a ***sql*** type undulating 2D network in the *ac*-plane, as depicted in Fig. 2b and c. The edge lengths, i.e. the Co···Co separation within the {Co$_4$(**BIX**)$_2$(**BrIP**)$_2$} rectangular grid are 10.18 and 14.16 Å; whereas, the diagonal Co···Co separations are 16.21 and 18.58 Å. The overall network topology could be described with the short vertex symbol 4^4. The 2D network viewed down the *a*-axis shows a zigzag pattern with perfect alignment of the ligand moieties within the 2D motif, as depicted in Fig. 2c. Within the 2D network {Co(II)**BrIP**}$_n$ linear

Table 2
Hydrogen bonding parameters for **1**.

D–H···A	d(H···A) (Å)	d(D···A) (Å)	∠D–H···A (°)
CP1			
C(9)–H(9)···O(3)$_1$	2.40(3)	3.19(3)	160(3)
C(20)–H(20)···O(2)$_2$	2.42(3)	3.26(3)	161(2)
C(12)–H(12B)···Br1$_3$	3.15(2)	3.97(2)	145(1)
C(22)–H(22)···Br1$_4$	3.12(3)	3.86(2)	140(2)
C(7)–H(7)···Br1$_5$	3.10(3)	4.02(2)	162.6(3)
C(11)–H(11)···Br1$_6$	3.16(2)	3.89(3)	151.1(2)

Symmetry codes: 1. $-x$, 1 − y, $-z$; 2. $-x$,1/2 + y,1/2 − z; 3. -1 + x,1/2 − y,$-1/2$ + z; 4. x,1 − y,$-z$; 5. $-x$,$-y$,$-z$; 6. $-x$,$-1/2$ + y,1/2 − z.

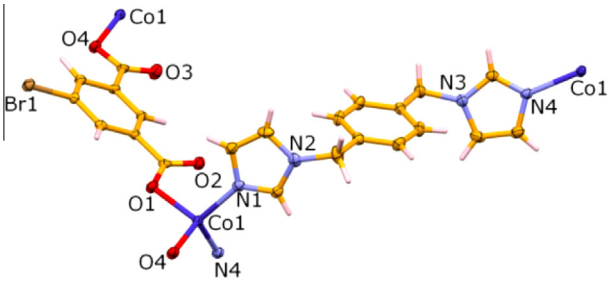

Fig. 1. ORTEP diagram depicting the coordination sphere with the atom numbering scheme for **1** (50% probability factor for the thermal ellipsoids).

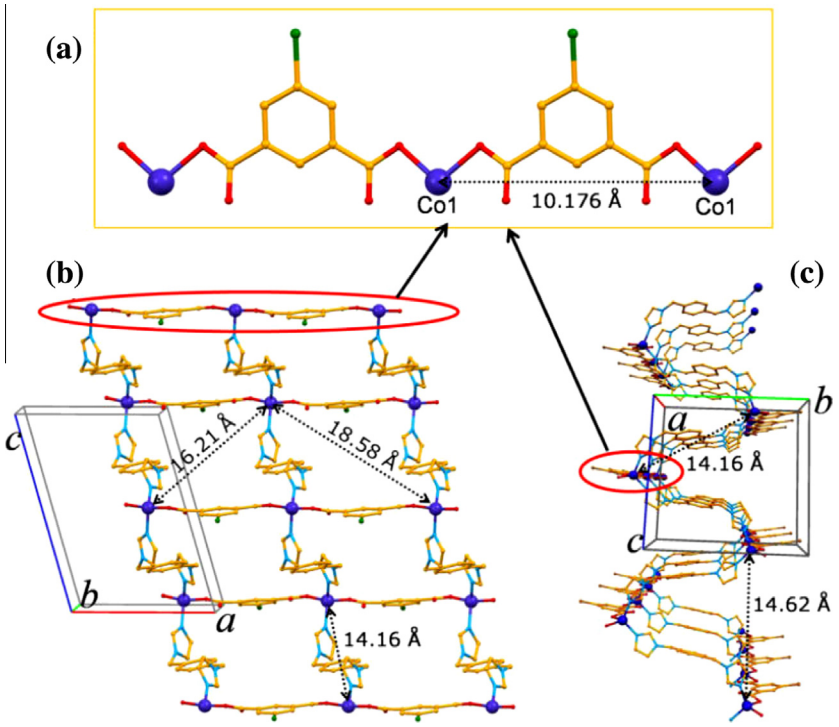

Fig. 2. (a) {Co(II)**BrIP**}$_n$ chain running along the *a*-axis; (b) ***sql*** type [Co(**BrIP**)(**BIX**)]$_n$ network with 16.21 × 18.58 Å^2 windows through which another such network interpenetrates; (c) deep undulated network constructed upon strategic connections between diagonal glide related {Co(II)**BrIP**}$_n$ chains *via* **BIX** molecules confined in an *anti*-conformation.

chains are stacked on each other down the *c*-axis in a completely eclipsing manner, with the Co···Co separation between the 1, 3 {Co(II)**BrIP**}$_n$ chains of the rectangular grid being 14.62 Å and 1, 2 {Co(II)**BrIP**}$_n$ chains being 14.16 Å. The close Co···Co separation distances of 1, 2 and 1, 3 {Co(II)**BrIP**}$_n$ chains evidently indicate the high degree of undulation of the 2D sheets, which is attributable to the conformational flexibility of the **BIX** moiety and distortion in the tetrahedral coordination environment around the Co(II) centers (Fig. 2c).

The packing diagram (Fig. 3) shows three independent 2D sheets interlocked with each other in a 'one up' and 'one down' pattern, resulting in a threefold parallel interpenetration of undulated ***sql*** networks. Interestingly, the dimensional increase from 2D sheets to an overall 3D entanglement, i.e. polycatenated 2D → 3D parallel interpenetration, observed in this case is a rarely observed structural feature. Highly acclaimed reviews by Carlucci et al. and Batten also call attention to the demanding geometrical prerequisites for the parallel interpenetration of networks to occur, which justify the fact that parallel interpenetration is a rarely observed kind of entanglement as compared to the inclined or perpendicular interpenetration [18]. Evidently, the conformational flexibility of the **BIX** moiety in **1** has played a crucial role in the realization of highly undulated sheets which in turn endure parallel interpenetration with a 2D → 3D dimensional extension. In an earlier relevant report, Liu and co-workers have also shown 2D → 3D parallel interpenetration resulting from 'deeper undulation' of 2D sheets [19].

In an attempt to understand the polycatenated 2D → 3D interpenetration, weak molecular interactions between the 2D networks in **1** were analyzed in detail. Interestingly, the polycatenated nets are involved in C–H···O interactions involving the uncoordinated carboxylate oxygen O3 and O2 of the **BrIP** ligand with the imidazole hydrogen atoms H9 and H20 of the **BIX** moiety, respectively, as presented in Fig. 4. In addition to this intermolecular H-bonding, a π···π interaction between the phenyl rings of the **BrIP** and **BIX** moieties with a perpendicular distance of 3.62(2) Å between the centroids of the phenyl rings was also observed (symmetry code: $-x, -1/2 + y, 1/2 - z$). The Br atom from the **BrIP** moiety is drawn in various intermolecular C–H···Br interactions between the imidazole hydrogen atoms H11 and H22, methylene hydrogen H12 of the **BIX** moiety and phenyl hydrogen H7 of the **BrIP** ligand with H···Br distances ranging from 3.10(2) to 3.16(2) Å. Details of the pertinent H-bonding interactions with their symmetry codes are given in Table 2. The aforementioned intermolecular interactions are also responsible for the polycatenation of the 2D nets and stabilization of the molecular structure in the crystal lattice.

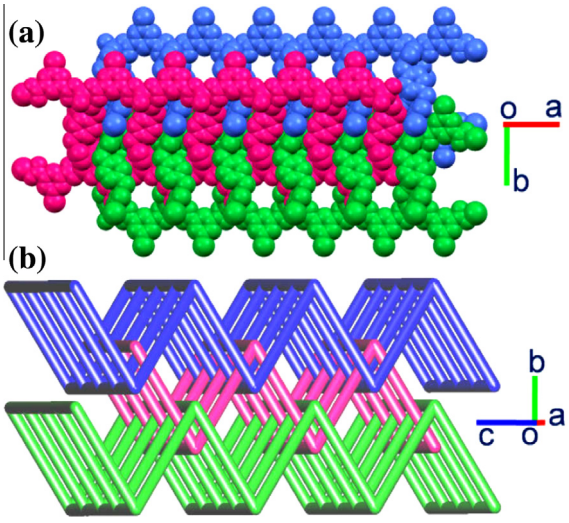

Fig. 3. (a) Threefold interpenetration of 2D metal organic networks in coordination polymer **1** presented down the *c*-axis; (b) simplified topological depiction of **1**.

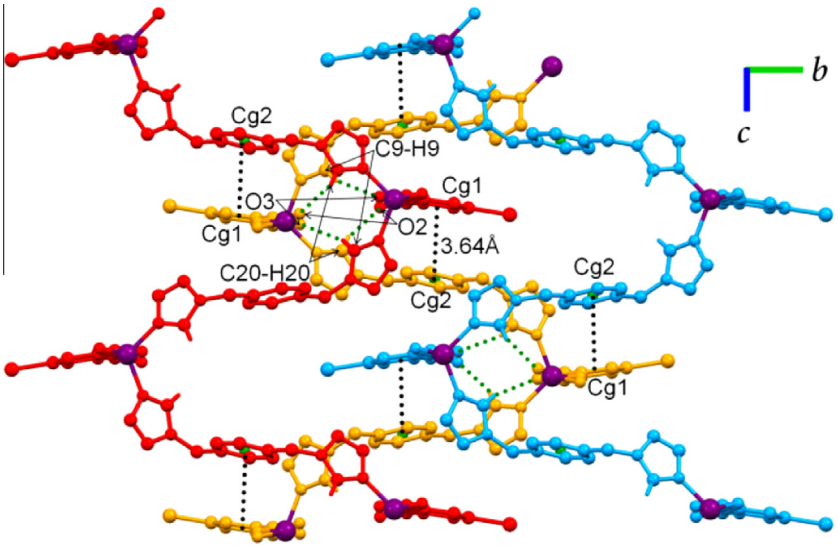

Fig. 4. Close-up view along the *a*-axis depicting three interlocked $[Co(\mathbf{BrIP})(\mathbf{BIX})]_n$ networks glued together by means of C–H···O hydrogen bonding and π···π interactions between the phenyl rings of **BrIP** and **BIX**.

3.2. Kneading experiments and PXRD analysis

Both isostructural CPs, **1** ($_{Nitrate}\mathbf{1}^{Neat}$, $_{Nitrate}\mathbf{1}^{MeOH}$, $_{Hydroxide}\mathbf{1}^{H_2O}$ and $_{Nitrate}\mathbf{1}^{H_2O}$) and **2** ($_{Nitrate}\mathbf{2}^{H_2O}$ and $_{Oxide}\mathbf{2}^{H_2O}$) were quickly and efficiently synthesized by kneading the stoichiometric ternary reaction mixture with or without a minute amount of solvent. Product formation commenced within few minutes of grinding, which could be assessed by the rapid development of a bright purple color in the case of the cobalt CP, **1**. Commencement of the reaction was further confirmed by comparing the immediately recorded PXRD patterns of the cobalt samples after 10 min. Neat and water assisted kneading with the simulated PXRD pattern of **1** and its constituents is presented in Fig. S1. It is evident that after 10 min of grinding, the patterns for the reaction mixtures no longer match with those of the precursors and a few peaks corresponding to the framework appeared. Neat grinding was continued for *ca.* 45 min, whereas liquid assisted grinding (LAG) was continued for a shorter duration of 15 to 20 min. Our observations support previous reports suggesting that the use of a small amount of solvent enhances the mobility of the reactants to yield the homogeneous product quickly [9]. In fact, we observed that when the nitrate salts of Co(II)/Zn(II) and organic linkers were kneaded under solvent free conditions, the product formation was slow (indicated by a color change in case of the Co CP), and required a longer kneading time (45 min.) to achieve the desired product (Fig. S2). It was also observed that the solvent free reaction between $Co(OH)_2$, **BIX** and H_2**BrIP** was too slow to yield the desired product, even after kneading for 60 min, whereas the solvent free grinding of ZnO with ligands under identical conditions resulted in the formation of $_{Oxide}\mathbf{2}^{Neat}$. The products synthesized by neat grinding were not phase pure and intense reflections of ZnO impurities were observed in the case of $_{Oxide}\mathbf{2}^{Neat}$ (Fig. 5).

Since neat grinding did not offer phase purity of synthesized **1** and **2**, we attempted LAG methods for synthesizing both CPs. A few drops of water or methanol were added to the reaction mixture, which on grinding for *ca* 15 min resulted in phase pure samples of $_{Nitrate}\mathbf{1}^{MeOH}$, $_{Hydroxide}\mathbf{1}^{H_2O}$, $_{Nitrate}\mathbf{1}^{H_2O}$, $_{Nitrate}\mathbf{2}^{H_2O}$ and $_{Oxide}\mathbf{2}^{H_2O}$. Rietveld refinements were performed for all samples of the Co CPs, which indicated the formation of phase pure samples with the LAG technique. Rietveld fits for $_{Nitrate}\mathbf{1}^{Neat}$, $_{Nitrate}\mathbf{1}^{MeOH}$, $_{Hydroxide}\mathbf{1}^{H_2O}$ and $_{Nitrate}\mathbf{1}^{H_2O}$ are presented in Fig. 6, and these indicate the formation of a ternary interpenetrated network of **1** in all cases. Agreement indices further indicate the phase purity of all the prepared samples, except $_{Nitrate}\mathbf{1}^{Neat}$. Refined lattice parameters for the samples of **1** synthesized *via* neat kneading and LAG routes are compared with those obtained from the single crystal structure solution of **1** in Table 3. It was further observed that brief washing of the synthesized CPs with methanol significantly improved the phase purity due to the removal of minor unreacted precursors, as evident from the PXRD data (Fig. 7).

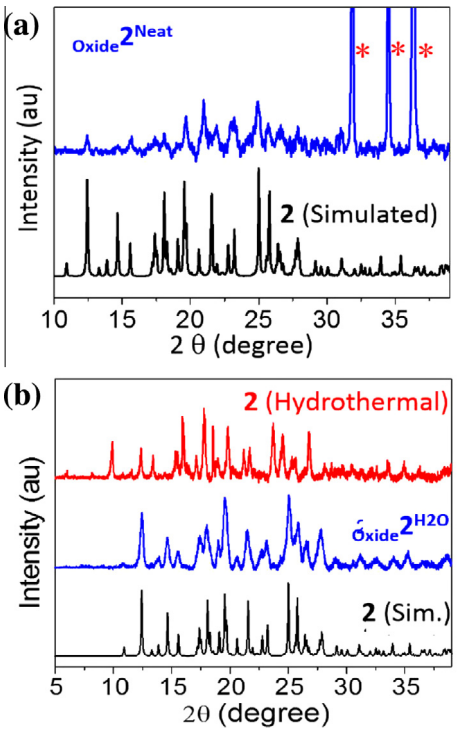

Fig. 5. A comparison between the simulated PXRD patterns of **2** and experimental patterns of $_{Oxide}\mathbf{2}^{Neat}$ indicate the presence of ZnO (reflections marked with an asterisk) as an impurity in $_{Oxide}\mathbf{2}^{Neat}$ (a); comparison of the simulated PXRD patterns of **2** with $_{Oxide}\mathbf{2}^{H_2O}$ and a solvothermally prepared sample (b).

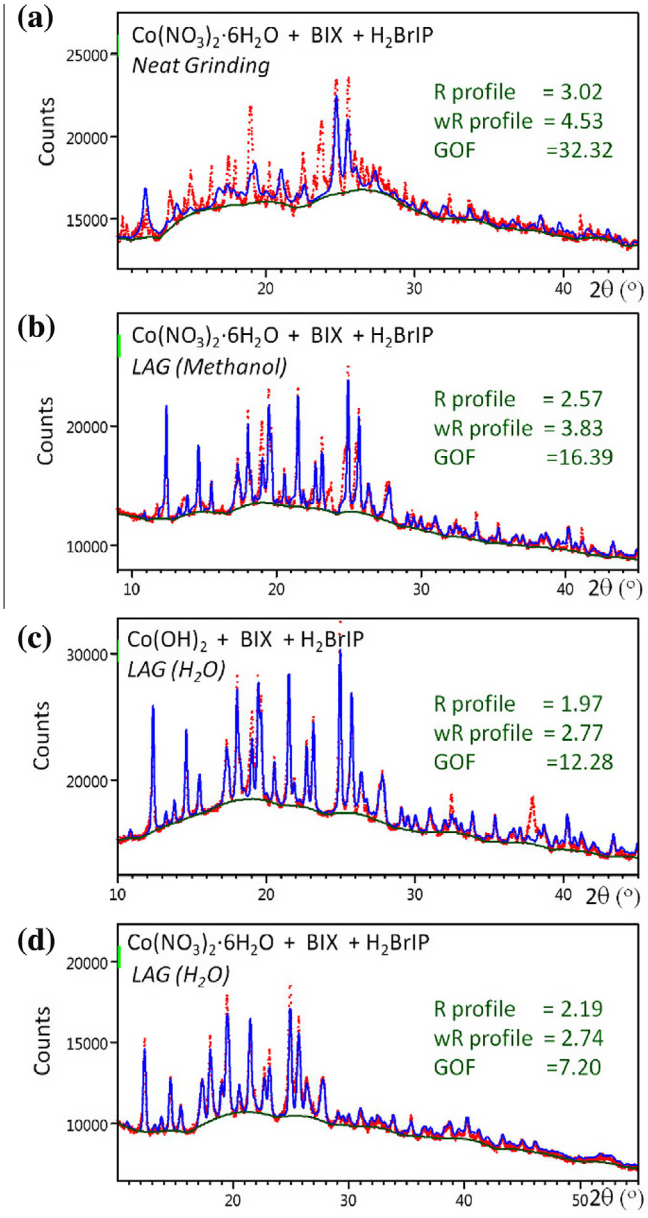

Fig. 6. Rietveld fits of experimental (red) and simulated (blue) PXRD patterns for $_{Nitrate}\mathbf{1}^{Neat}$ (a), $_{Nitrate}\mathbf{1}^{MeOH}$ (b), $_{Hydroxide}\mathbf{1}^{H_2O}$ (c) and $_{Nitrate}\mathbf{1}^{H_2O}$ (d). (Color online.)

Table 3
Comparison of the lattice parameters obtained from single crystal structure solution and Rietveld fitting of experimental PXRD patterns of $_{Nitrate}\mathbf{1}^{Neat}$, $_{Nitrate}\mathbf{1}^{MeOH}$, $_{Hydroxide}\mathbf{1}^{H_2O}$ and $_{Nitrate}\mathbf{1}^{H_2O}$.

Sample	*a* (Å)	*b* (Å)	*c* (Å)	*β* (°)
Single crystal	10.176	14.367	14.624	106.034
$_{Nitrate}\mathbf{1}^{Neat}$	10.143	14.249	14.518	105.943
$_{Nitrate}\mathbf{1}^{MeOH}$	10.180	14.408	14.775	105.257
$_{Hydroxide}\mathbf{1}^{H_2O}$	10.161	14.401	14.753	105.309
$_{Nitrate}\mathbf{1}^{H_2O}$	10.154	14.372	14.743	105.202

3.3. Scanning electron microscopy and EDX analysis

Scanning electron microscopy (SEM) was utilized to analyze the textural features of **1** and **2** synthesized *via* different routes (Figs. 8 and S3). CP **1** prepared by the hydrothermal method showed rod-like tiny crystals aggregated in solid spherical shapes having *ca.*

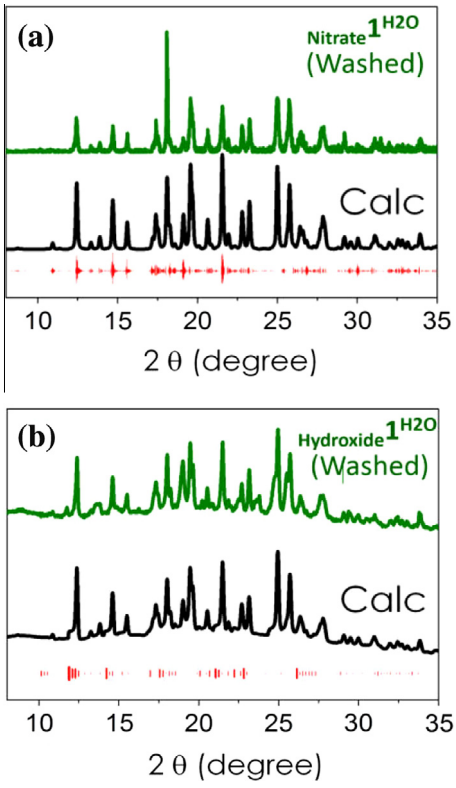

Fig. 7. Comparison between the simulated PXRD pattern of **1** and experimental patterns recorded for the methanol washed $_{Nitrate}\mathbf{1}^{H_2O}$ (a) and $_{Hydroxide}\mathbf{1}^{H_2O}$ (b), indicating that the washing significantly improved the phase purity. The difference between the simulated and experimental patterns is plotted in red. (Color online.)

12–15 μm diameter. Neat grinding resulted in rectangular flake shaped crystals (length *ca.* 1 μm) which on washing gave smaller crystalline particles with an average dimension of 0.5 μm. Similarly samples of $_{Hydroxide}\mathbf{1}^{H_2O}$ and $_{Nitrate}\mathbf{1}^{H_2O}$ prepared by the LAG method showed tiny particles with an average dimension of 0.5 μm. No specific aggregation pattern was observed for samples prepared by neat kneading or water assisted grinding methods. However, the methanol assisted grinding resulted in rod-like tiny crystals aggregated in solid spherical shapes having *ca.* 12–15 μm diameter, as in the case of **1** synthesized by the hydrothermal method.

The textural features of the Zn CP samples prepared *via* different routes were similar to their Co counterparts. Hence, rod-like structures aggregated into spherical assemblies were observed for **2** prepared from the hydrothermal and methanol assisted grinding methods, whereas the water assisted grinding resulted in tiny crystalline particles lacking a confined shape. Energy-dispersive X-ray spectroscopy (EDX) provided valuable information about the composition of the materials synthesized using different methods (Fig. S4). Single crystal data revealed the molecular formula of the repeating unit of **1** to be $CoC_{22}H_{17}BrN_4O_4$. Thus the relative composition of the elements carbon and cobalt in CP **1** is: C, 81.76% and Co, 18.24%. EDX analysis indicated that the C/Co ratio remains at 75.57/24.43 for **1** prepared hydrothermally, 75.49/24.51 for $_{Nitrate}\mathbf{1}^{H_2O}$ and 75.22/24.78 for $_{Nitrate}\mathbf{1}^{MeOH}$. These values are pretty close to the expected ones and were consistent from different sites of the prepared samples. The C/Co ratio for the sample synthesized by neat grinding varied in the range 78.88/21.12 to 63.05/36.95 at different sites of the sample under observation. This inconsistency in the observed elemental composition is attributable to minute amounts of unreacted precursors. Similar EDX analysis was performed for **2**, giving a 80.16/19.84 ratio for the C/Zn elements. The observed C/Zn values were in the range

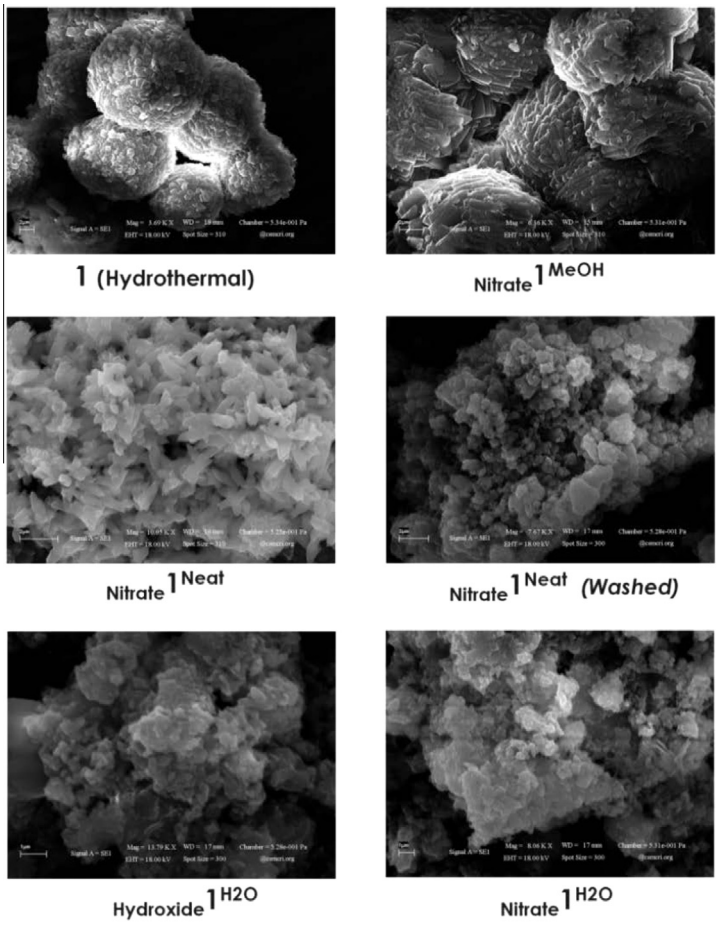

Fig. 8. SEM micrographs of Co CP, **1** prepared *via* different synthetic methodologies. The morphological resemblance between **1** (hydrothermal) and $_{Nitrate}\mathbf{1}^{MeOH}$ is noteworthy.

78.49/21.51 to 76.25/23.75 for samples synthesized by the hydrothermal and LAG methods. As in case of $_{Nitrate}\mathbf{1}^{Neat}$, the compositions of $_{Nitrate}\mathbf{2}^{Neat}$ and $_{Oxide}\mathbf{2}^{Neat}$ were also inconsistent at different sites of the sample under examination.

3.4. TGA and FTIR

Co CP **1**, prepared from the hydrothermal method as well as the LAG method, showed thermal stability up to 300 °C, which is equivalent to the thermal stability of the previously reported Zn CP **2** (Fig. S5). Beyond 300 °C the frameworks initially show gradual weight loss and after 350 °C rapid weight loss, indicating the thermal decomposition of the framework.

Co CP derived from hydrothermal and mechanochemical methods showed FTIR spectra which furnished complementary information to the crystallographic findings (Fig. S6). Asymmetric and symmetric C=O stretching modes of the carboxylate moiety were observed as medium intensity bands at *ca.* 1616 and 1554 cm^{-1} respectively for all samples, attributable to the $\mu_1\eta^1$ coordination mode of each carboxylate group of the **BrIP** dianion. A sharp band at *ca.* 1345 cm^{-1} for the aromatic C=N stretch of **BIX** was consistently observed in all samples, irrespective of the synthetic methodology adopted to prepare them. Weak bands at *ca.* 729, 658 and 438 cm^{-1} may be attributed to the Co–N and Co–O vibrational modes.

3.5. Absorption and emission spectra

Solid state absorption spectra were recorded at room temperature with a non-polarized light source for Co and Zn CPs as well as the ligands (Fig. S7). The free ligands H_2**BrIP** and **BIX** absorb at 300 and 267 nm respectively whereas both CPs showed absorption maxima at ca. 300 nm. An additional low intensity band in the case of Co CP was observed at 578 nm and assigned to the *d–d* band; this was responsible for the violet color of the compound. The absorption bands at 302 nm and lower wavelengths observed for **1** and **2** are attributed to π–π^* and n–π^* ligand field transitions. The Co CP materials synthesized *via* different methods showed identical spectral features as for **1** synthesized by the hydrothermal method.

The emission behavior of **1** and **2** was studied in the solid state at room temperature and the emission spectra are presented in Fig. S8. **1** and **2** prepared by the solvothermal and LAG methods showed similar emission profiles, comprising two emission bands at *ca* 325 and 425 nm upon excitation by an absorbance wavelength of 302 nm; however, the emission intensity of **2** was higher than that observed for **1**. The emission profiles of the free ligands **BIX** and **H_2BrIP** were also recorded and these showed strong emission bands at 416 and 507 nm respectively, as presented in Fig. S8. A comparison of the 425 nm band observed for **1** and **2** with the strong emission of **BIX** at 416 nm suggests a metal perturbed ligand field emission for both CPs.

4. Conclusion

A ternary Co CP, $[Co(\mathbf{BIX})(\mathbf{BrIP})]_n$ (**1**), which possesses intriguing threefold parallel interpenetration of 2D ***sql*** networks has been prepared hydrothermally as well as *via* various mechanochemical methods. Single crystals of the material were obtained hydrothermally and the structure solution revealed that CP **1** is isostructural

to a previously known Zn CP, $[Zn(\mathbf{BIX})(\mathbf{BrIP})]_n$ (**2**), which was synthesized by a different solvothermal protocol. Neat grinding and liquid assisted grinding in the presence of water or methanol showed a rapid synthesis of these materials. Most efficient results were obtained for methanol assisted grinding in the case of nitrate salts of the employed metal ions. However, $Co(OH)_2$ and ZnO also yielded the desired products when kneaded in the presence of a minute amount of water, offering an environmentally friendly method as the side product was only water in either case. The product formation in each mechanochemical case was confirmed by PXRD techniques and Rietveld refinement was performed in the case of the Co samples, which showed good agreement of the unit cell parameters between the materials synthesized by the hydrothermal and mechanochemical methods. Both the synthesized CPs showed thermal stability up to 300 °C, irrespective of the synthetic protocol that was followed. Supramolecular arrangements of self-assembled components *via* mechanochemistry entail a higher level of complexity and sophistication which presently are beyond our grasp. However, the results reported here not only present an example to advocate the scope of mechanochemistry towards intricate coordination polymeric architectures, but may also serve to increase our understanding of the entanglement processes in the solid state involving ternary supramolecular assemblies.

Acknowledgments

Authors acknowledge the CSIR India (HYDEN Project Grant No. CSC 0122) for financial support, Ms. Riddhi Laiya for XRPD data, Mr. Gaurav Vyas for TGA data, Mr. V.K. Agrawal for IR data, Mr. Viral Vakani for CHN analysis and Dr. P. Paul for all round analytical support. K.K.B. acknowledges CSIR (India) for a senior research fellowship. Publication Registration Number: CSIR-CSMCRI 111/2014.

Appendix A. Supplementary data

CCDC 977334 contains the supplementary crystallographic data for **1**. These data can be obtained free of charge via http://www.ccdc.cam.ac.uk/conts/retrieving.html, or from the Cambridge Crystallographic Data Centre, 12 Union Road, Cambridge CB2 1EZ, UK; fax: (+44) 1223-336-033; or e-mail: deposit@ccdc.cam.ac.uk. Supplementary data associated with this article can be found, in the online version, at http://dx.doi.org/10.1016/j.poly.2014.10.029.

References

[1] (a) K.D.M. Harris, Nat. Chem. 5 (2013) 12;
(b) T. Friščić, D.G. Reid, I. Halasz, R.S. Stein, R.E. Dinnebier, M.J. Duer, Angew. Chem., Int. Ed. 49 (2010) 712;
(c) G. Kaupp, CrystEngComm 11 (2009) 388;
(d) K. Ralphs, C. Hardacre, S.L. James, Chem. Soc. Rev. 42 (2013) 7701;
(e) R.B.N. Baig, R.S. Varma, Chem. Soc. Rev. 41 (2012) 1559.
[2] (a) D. Braga, M. Curzi, A. Johansson, M. Polito, K. Rubini, F. Grepioni, Angew. Chem., Int. Ed. 45 (2006) 142;
(b) J.C. Crittenden, H.S. White, J. Am. Chem. Soc. 132 (2010) 4503;
(c) M. Balaz, P. Balaz, M.J. Sayagues, A. Zorkovska, Mater. Sci. Semicond. Process. 16 (2013) 1899;
(d) D.V. Onishchenko, Mater. Sci. 49 (2013) 220;
(e) O.A. Knyazheva, O.N. Baklanova, A.V. Lavrenov, V.A. Drozdov, N.N. Leont'eva, A.V. Vasilevich, A.V. Shilova, V.A. Likholobov, Kinet. Catal. 55 (2014) 121;
(f) S. Heiden, L. Tröbs, K.J. Wenzel, F. Emmerling, CrystEngComm 14 (2012) 5128;
(g) T. Kleine, J. Buendia, C. Bolm, Green Chem. 15 (2013) 160;
(h) A.V. Trask, D.A. Haynes, W.D.S. Motherwell, W. Jones, Chem. Commun. (2006) 51;
(i) D.R. Weyna, T. Shattock, P. Vishweshwar, M.J. Zaworotko, Cryst. Growth Des. 9 (2009) 1106;
(j) M. Cindrić, M. Uzelac, D. Cinčić, I. Halasz, G. Pavlović, T. Hrenar, M. Ćurić, D. Kovačević, CrystEngComm 14 (2012) 3039;
(k) E. Batisai, M. Lusi, T. Jacobs, L.J. Barbour, Chem. Commun. 48 (2012) 12171.
[3] (a) A.A.L. Michalchuk, I.A. Tumanov, E.V. Boldyreva, CrystEngComm 15 (2013) 6403;
(b) E. Boldyreva, Chem. Soc. Rev. 42 (2013) 7719;
(c) E.A. Losev, E.V. Boldyreva, CrystEngComm 16 (2014) 3857.
[4] S.H. Lapidus, A. Naik, A. Wixtrom, N.E. Massa, V. Ta Phuoc, L. del Campo, S. Lebegue, J.G. Angyan, T. Abdel-Fattah, S. Pagola, Cryst. Growth Des. 14 (2014) 91;
(b) F.C. Gennari, J. Alloys Compd. 581 (2013) 192;
A.I. Ramos, T.M. Braga, P. Silva, J.A. Fernandes, P. Ribeiro-Claro, M. de Fatima Silva Lopes, F.A.A. Paz, S.S. Braga, CrystEngComm 15 (2013) 2822;
(d) J. Yoshida, S. Nishikiori, R. Kuroda, H. Yuge, Chem. Eur. J. 19 (2013) 3451;
(e) M. Arhangelskis, G.O. Lloyd, W. Jones, CrystEngComm 14 (2012) 5203;
(f) D. Cinčić, T. Friščić, W. Jones, J. Am. Chem. Soc. 130 (2008) 7524;
(h) K. Chadwick, R. Davey, W. Cross, CrystEngComm 9 (2007) 732.
[5] (a) C. Mottillo, Y. Lu, M.H. Pham, M.J. Cliffe, T.O. Do, T. Friščić, Green Chem. 15 (2013) 2121;
(b) J. Stojaković, B.S. Farris, L.R. MacGillivray, Chem. Commun. 48 (2012) 7958;
(c) D. Prochowicz, I. Justyniak, A. Kornowicz, T. Kaczorowski, Z. Kaszkur, J. Lewiński, Chem. Eur. J. 18 (2012) 7367;
(d) A. Pichon, S.L. James, CrystEngComm 10 (2008) 1839;
(e) N.K. Singh, M. Hardi, V.P. Balema, Chem. Commun. 49 (2013) 972;
(f) P.J. Beldon, L. Fábián, R.S. Stein, A. Thirumurugan, A.K. Cheetham, T. Friščić, Angew. Chem., Int. Ed. 49 (2010) 9640.
[6] (a) S.L. James, C.J. Adams, C. Bolm, D. Braga, P. Collier, T. Friščić, F. Grepioni, K.D.M. Harris, G. Hyett, W. Jones, A. Krebs, J. Mack, L. Maini, A.G. Orpen, I.P. Parkin, W.C. Shearouse, J.W. Steed, D.C. Waddelli, Chem. Soc. Rev. 41 (2012) 413;
(b) D.J.C. Constable, P.J. Dunn, J.D. Hayler, G.R. Humphret, J.L. Leazer Jr., R.J. Linderman, K. Lorenz, J. Manley, B.A. Pearlman, A. Wells, A. Zaks, T.Y. Zhang, Green Chem. 9 (2007) 411;
(c) W.J.W. Watson, Green Chem. 14 (2012) 251;
(d) P. Anastas, N. Eghbali, Chem. Soc. Rev. 39 (2010) 301;
(e) A. Pichon, A. Lazuen-Garay, S.L. James, CrystEngComm 8 (2006) 211;
(f) V. Safarifard, A. Morsali, CrystEngComm 14 (2012) 5130;
(g) M. Nagarathinam, A. Chanthapally, S.H. Lapidus, P.W. Stephens, J.J. Vittal, Chem. Commun. 48 (2012) 2585;
(h) C. Jobbágy, T. Tunyogi, G. Pálinkás, A. Deák, Inorg. Chem. 50 (2011) 7301;
(i) K. Fujii, A.L. Garay, J. Hill, E. Sbircea, Z. Pan, M. Xu, D.C. Apperley, S.L. James, K.D.M. Harris, Chem. Commun. 46 (2010) 7572;
(j) M. Klimakow, P. Klobes, K. Rademann, F. Emmerling, Microporous Mesoporous Mater. 154 (2012) 113.
[7] W.J. Belcher, C.A. Longstaff, M.R. Neckening, J.W. Steed, Chem. Commun. (2002) 1602.
[8] (a) D. Braga, F. Grepioni, Angew. Chem., Int. Ed. 43 (2004) 4002;
(b) A.L. Garay, A. Pichon, S.L. James, Chem. Soc. Rev. 36 (2007) 846;
(c) D. Braga, S.L. Giaffreda, F. Grepioni, A. Pettersen, L. Maini, M. Curzi, M. Polito, Dalton Trans. (2006) 1249;
(d) M. Ferguson, N. Giri, X. Huang, D. Apperley, S.L. James, Green Chem. 16 (2014) 1374.
[9] (a) T. Friščić, I. Halasz, V. Strukil, M. Eckert-Maksic, R.E. Dinnebier, Croat. Chem. Acta 85 (2012) 367;
(b) T. Friščić, W. Jones, Cryst. Growth Des. 9 (2009) 1621;
(c) G.A. Bowmaker, Chem. Commun. 49 (2013) 334;
(d) D. Braga, S.L. Giaffreda, F. Grepioni, M.R. Chierotti, R. Gobetto, G. Palladinoa, M. Polito, CrystEngComm 9 (2007) 879;
(e) J. Bonnamour, T.X. Métro, J. Martinez, F. Lamaty, Green Chem. 15 (2013) 1116;
(f) D. Braga, L. Maini, S.L. Giaffreda, F. Grepioni, M.R. Chierotti, R. Gobetto, Chem. Eur. J. 10 (2004) 3261.
[10] T. Friščić, Chem. Soc. Rev. 41 (2012) 3493.
[11] (a) P.K. Thallapally, J. Tian, M.R. Kishan, C.A. Fernandez, S.J. Dalgarno, P.B. McGrail, J.E. Warren, J.L. Atwood, J. Am. Chem. Soc. 130 (2008) 16842;
(b) Y. Feng, H. Jiang, M. Chen, Y. Wang, Powder Technol. 249 (2013) 38;
(c) L. Wen, P. Cheng, W. Lin, Chem. Sci. 3 (2012) 2288.
[12] T. Friščić, L. Fabian, CrystEngComm 11 (2009) 743.
[13] (a) G. Koshkakaryan, L.M. Klivansky, D. Cao, M. Snauko, S.J. Teat, J.O. Struppe, Y. Liu, J. Am. Chem. Soc. 131 (2009) 2078;
(b) G.W. Wang, Chem. Soc. Rev. 42 (2013) 7668;
(c) S.Y. Hsueh, K.W. Cheng, C.C. Lai, S.H. Chiu, Angew. Chem., Int. Ed. 47 (2008) 4436.
[14] H. Furukawa, K.E. Cordova, M. O'Keeffe, O.M. Yaghi, Science 341 (2013) 1230444.
[15] G.X. Liu, K. Zhu, S. Nishihara, R.Y. Huang, X.M. Ren, Inorg. Chim. Acta 362 (2009) 5103.
[16] (a) J. Yang, H. Liu, W.N. Martens, R.L. Frost, J. Phys. Chem. C 114 (2010) 111;
(b) B.F. Abrahams, B.F. Hoskins, R. Robson, D.A. Slizys, Acta Crystallogr., Sect. C 54 (1998) 1666;
(c) K. Rajesh, M. Somasundaram, R. Saiganesh, K.K. Balasubramanian, J. Org. Chem. 72 (2007) 5867.
[17] (a) G.M. Sheldrick, SAINT 5.1 ed., Siemens Industrial Automation Inc., Madison, WI, 1995;
(b) SADABS, Empirical Absorption Correction Program, University of Göttingen, Göttingen, Germany, 1997.;
(c) G.M. Sheldrick, SHELXTL Reference Manual: Version 5.1, Bruker AXS, Madison, WI, 1997;
(d) G.M. Sheldrick, SHELXL-97: Program for Crystal Structure Refinement, University of Göttingen, Göttingen, Germany, 1997.
[18] (a) L. Carlucci, G. Ciani, D.M. Proserpio, Coord. Chem. Rev. 246 (2003) 247;
(b) S.R. Batten, CrystEngComm 18 (2001) 1.
[19] F.Q. Liu, T.D. Tilley, Inorg. Chem. 36 (1997) 5090.